
VIVAT: VIRTUOUS IMPROVING VAE TRAINING THROUGH ARTIFACT MITIGATION

Lev Novitskiy^{1,*},

Viacheslav Vasilev¹,

Maria Kovaleva¹,

Vladimir Arkhipkin¹,

Denis Dimitrov¹

¹Kandinsky Lab, Moscow, Russia

*Corresponding author: levnovitskiy@gmail.com

ABSTRACT

Variational Autoencoders (VAEs) remain a cornerstone of generative computer vision, yet their training is often plagued by artifacts that degrade reconstruction and generation quality. This paper introduces VIVAT, a systematic approach to mitigating common artifacts in KL-VAE training without requiring radical architectural changes. We present a detailed taxonomy of five prevalent artifacts – color shift, grid patterns, blur, corner and droplet artifacts – and analyze their root causes. Through straightforward modifications, including adjustments to loss weights, padding strategies, and the integration of Spatially Conditional Normalization, we demonstrate significant improvements in VAE performance. Our method achieves state-of-the-art results in image reconstruction metrics (PSNR and SSIM) across multiple benchmarks and enhances text-to-image generation quality, as evidenced by superior CLIP scores. By preserving the simplicity of the KL-VAE framework while addressing its practical challenges, VIVAT offers actionable insights for researchers and practitioners aiming to optimize VAE training.

1 Introduction

Variational Autoencoders (VAEs) [21, 37] have long been established as a cornerstone of generative AI, playing a pivotal role in tasks such as image reconstruction and image generation [52, 36, 46, 12, 54]. Their significance is further emphasized by their integration into modern latent diffusion pipelines [38, 7, 11, 25, 32, 1, 49, 6], where they serve as the main ingredient for latent space formation. Despite their widespread adoption and extensive research history, the training of high-quality VAEs remains fraught with challenges, particularly with respect to the emergence of artifacts that degrade generation quality [24, 42]. These persistent issues underscore the continued relevance of refining VAE training methodologies to enhance their robustness and generative fidelity.

Previous research has explored various architectural modifications and different concepts of VAEs, leading to the development of specialized model families and various changes in the optimization procedure [17, 47, 36, 39, 46, 8, 18, 30, 6, 24]. Although these contributions have expanded the theoretical understanding of VAEs, many works focus on fundamental innovations while neglecting practical considerations, particularly the systematic analysis and mitigation of training artifacts. Consequently, despite the diversity of proposed solutions, there remains a lack of straightforward and actionable strategies to address anomalies in existing VAE implementations and training process. In this work, we conduct a comprehensive classification and analysis of these artifacts, offering practical, easy-to-implement recommendations to eliminate them without resorting to radical architectural overhauls.

We posit that the potential of conventional autoencoding frameworks remains underutilized and that significant improvements can be achieved through targeted refinements rather than entirely new methodologies. To this end, we adopt the classic KL-VAE ¹ architecture [21] – a proven and widely used framework that has been successfully

¹Later in this paper, the terms “VAE” and “KL-VAE” will be used interchangeably, unless otherwise stated.

applied in prior work for modern generative models [7, 25, 11]. By systematically investigating the origins of training artifacts within this architecture, we propose simple yet effective solutions that yield measurable improvements in model performance. Quantitative evaluations demonstrate that our approach achieves state-of-the-art results for reconstruction quality without introducing unnecessary complexity or departing from established VAE training principles. With this work, we aim to provide valuable insights for researchers and practitioners who are seeking to optimize VAE training while preserving the simplicity and efficiency of classical autoencoding methods.

Thus, the key contributions of this work are as follows:

- We provide a detailed taxonomy of five common artifacts in KL-VAE training, identifying their potential root causes and their impact on reconstruction quality;
- We propose straightforward, easy-to-implement modifications to mitigate these artifacts, ensuring a stable training process without requiring fundamental architectural changes;
- We demonstrate that our approach enhances VAE performance, achieving superior results in reconstruction quality while maintaining the simplicity of the KL-VAE framework;
- Finally, we show that VAE, trained according to our methodology, is well-suited for the text-to-image generation task and demonstrates a high-level quality that surpasses the previous state-of-the-art image reconstruction model, namely Flux VAE [25], in terms of CLIP score.

This paper is organized as follows: In Section 3.1, we provide a brief overview of classic KL-VAE and the training losses used in our work. We then describe the basic KL-VAE architecture without any improvements in Section 3.2. Finally, we briefly mention the role of VAE in the image generation pipeline in Section 3.3. Section 4 focuses on common issues that arise during KL-VAE training and the reasons behind them. Section 5 presents our proposed solutions to these problems, while Section 6 presents the results of our improved method for image reconstruction and text-to-image generation.

2 Related works

2.1 VAE and its modifications

The classical VAE, also referred to as KL-VAE, was introduced by [21] and quickly adopted for conditional image generation [52]. The core principle of this approach involves minimizing the Kullback-Leibler (KL) divergence between the latent distribution and a Gaussian prior. Since its inception, this architecture has been widely utilized and extensively modified. Notable architectural innovations include hierarchical VAE [46] and DiffuseVAE [30], the latter employing diffusion processes to refine the blurry VAE outputs. Previous research has also explored the impact of architectural depth in autoencoders [8] and proposed a VAE variant optimized for high compression ratios (up to $128\times$) [6]. However, the majority of prior work has focused on developing novel loss functions and regularization techniques, such as spectral regularization [46], frequency-domain optimization [18], the integration of Wasserstein distance [44], and more [17, 39, 24, 42, 10, 43, 41, 56]. Despite these advancements, most of these contributions have not been widely adopted in large-scale commercial generative models. An alternative approach, VQ-VAE [47], replaces the continuous latent space with a discrete codebook, leading to significant improvements in generative tasks [36, 12, 54, 1]. This method has inspired numerous subsequent modifications [36, 57], including VQ-GAN [12], which enhances VQ-VAE through adversarial and perceptual losses. Nevertheless, quantized VAEs are known to produce geometric artifacts, and scaling their latent space dimensions is non-trivial. As a result, KL-VAE remains prevalent in several recent high-profile generative models [7, 11, 25]. In this work, we further investigate the KL-VAE architecture, aiming to advance its practical potential in reconstruction and generative applications.

2.2 VAE for latent diffusion

Due to inherent limitations in sample quality, VAEs are not the best option for generation tasks on their own. However, they have become a prominent component in latent diffusion models [38]. By reducing the spatial dimensions of images, VAEs enable more efficient representations, replacing computationally expensive pixel-based approaches. Latent diffusion models for image generation employ both continuous KL-VAEs [7, 11, 25] and quantized autoencoders [35, 1]. Key principles include increasing the channel size of latent variables and spatial compression ratios. When extending diffusion pipelines to video generation, modified VAEs were developed to incorporate temporal dependencies, either by preserving channel dimensions [5, 2] or compressing along the temporal axis [53, 23]. Since video VAEs build upon the image VAEs, our work focuses on analyzing spatial artifacts in image reconstruction, without loss of generality for the proposed solutions.

2.3 VAE artifacts

The problem of artifacts in image reconstruction using VAEs has been widely studied. A well-known limitation of VAEs is their tendency to produce blurred outputs, attributed to the asymmetric nature of the KL divergence [22]. While adversarial loss can mitigate blurring, it often introduces visual artifacts [26] and training instability, particularly at high resolutions [6]. Additionally, VAEs are prone to losing high-frequency information [18]. Stronger regularization (e.g., increasing the KL-divergence weight) yields a smoother latent space but reduces its information capacity, leading to loss of fine details and degraded reconstruction quality [24, 45]. Numerous studies have proposed improved training methods to reduce artifacts, yet most lack a systematic analysis or taxonomy of the specific visual artifacts encountered [39, 12, 18, 30]. [24] highlights a connection between artifacts and insufficient equivariance in the latent space under spatial transformations, though without explicitly categorizing the artifacts. Recently, visual artifacts in VAEs outputs have also been discussed in the context of diffusion-based generation pipelines. [42] notes that high-frequency components in VAE latent spaces can propagate undesirable artifacts into the final RGB images. In this work, we systematize common and problematic artifacts in VAE reconstructions and propose simple, effective mitigation strategies that require neither extensive changes to the training process nor fundamental modifications of the VAE architecture.

3 Preliminaries

3.1 VAE principles and objectives

The Variational Autoencoder (VAE) [21] is a generative model that learns latent representations of observed data \mathbf{x} through an encoder-decoder architecture. The encoder network parameterizes the approximate posterior distribution $q_\phi(\mathbf{z}|\mathbf{x})$ with weights ϕ , mapping input data to a latent space typically assumed Gaussian, while the decoder network parameterizes the likelihood $p_\theta(\mathbf{x}|\mathbf{z})$ with weights θ , reconstructing data from latent samples \mathbf{z} . The prior over the latent space $p(\mathbf{z})$ is usually chosen as a standard normal distribution $\mathcal{N}(\mathbf{0}, \mathbf{I})$. The VAE optimizes the evidence lower bound (ELBO), which balances reconstruction accuracy and latent space regularization:

$$\log p(\mathbf{x}) \geq \mathbb{E}_{q_\phi(\mathbf{z}|\mathbf{x})} \log p_\theta(\mathbf{x}|\mathbf{z}) - D_{\text{KL}}(q_\phi(\mathbf{z}|\mathbf{x}) \parallel p(\mathbf{z})) \quad (1)$$

Here, $\log p_\theta(\mathbf{x}|\mathbf{z})$ is the reconstruction term, ensuring that decoded samples match the input data, while the KL divergence D_{KL} encourages the learned posterior $q_\phi(\mathbf{z}|\mathbf{x})$ to align with the prior $p(\mathbf{z})$.

The VAE training objective combines several loss components that ensure proper latent space regularization and high-quality reconstructions. Modern VAE training setup requires several losses:

KL Divergence Loss [21]. The KL divergence term regularizes the latent space by minimizing the distance between the approximate posterior $q_\phi(\mathbf{z}|\mathbf{x})$ and the prior $p(\mathbf{z}) = \mathcal{N}(\mathbf{0}, \mathbf{I})$:

$$\mathcal{L}_{\text{KL}} = D_{\text{KL}}(q_\phi(\mathbf{z}|\mathbf{x}) \parallel p(\mathbf{z})). \quad (2)$$

For Gaussian distributions, this has closed-form solution:

$$\mathcal{L}_{\text{KL}} = -\frac{1}{2} \sum_{j=1}^J (1 + \log \sigma_j^2 - \mu_j^2 - \sigma_j^2), \quad (3)$$

where μ_j and σ_j are the mean and variance of the encoder’s posterior approximation.

Reconstruction Loss [21]. The reconstruction term ensures fidelity between input \mathbf{x} and output $\hat{\mathbf{x}} = p_\theta(\mathbf{x}|\mathbf{z})$. For continuous data (MSE):

$$\mathcal{L}_{\text{recon}} = \mathbb{E}_{q_\phi(\mathbf{z}|\mathbf{x})} \|\mathbf{x} - \hat{\mathbf{x}}\|_2^2. \quad (4)$$

Adversarial Loss [26]. Regular reconstruction losses in practice often lead to blurry reconstructions. This fact is worsen by the KL term which regularizes the latent space and negatively effects the reconstruction quality. When combined with GAN framework, the adversarial loss improves sample quality:

$$\mathcal{L}_{\text{adv}} = \mathbb{E}_{q_\phi(\mathbf{z}|\mathbf{x})} \log(1 - D(\hat{\mathbf{x}})), \quad (5)$$

where D is a discriminator network trained to distinguish real from generated samples. The discriminator helps automatically detect specific details that VAE fails to reconstruct, unlike the reconstruction loss. Moreover models finetuned with an adversarial loss have proved to have higher alignment with human preferences.

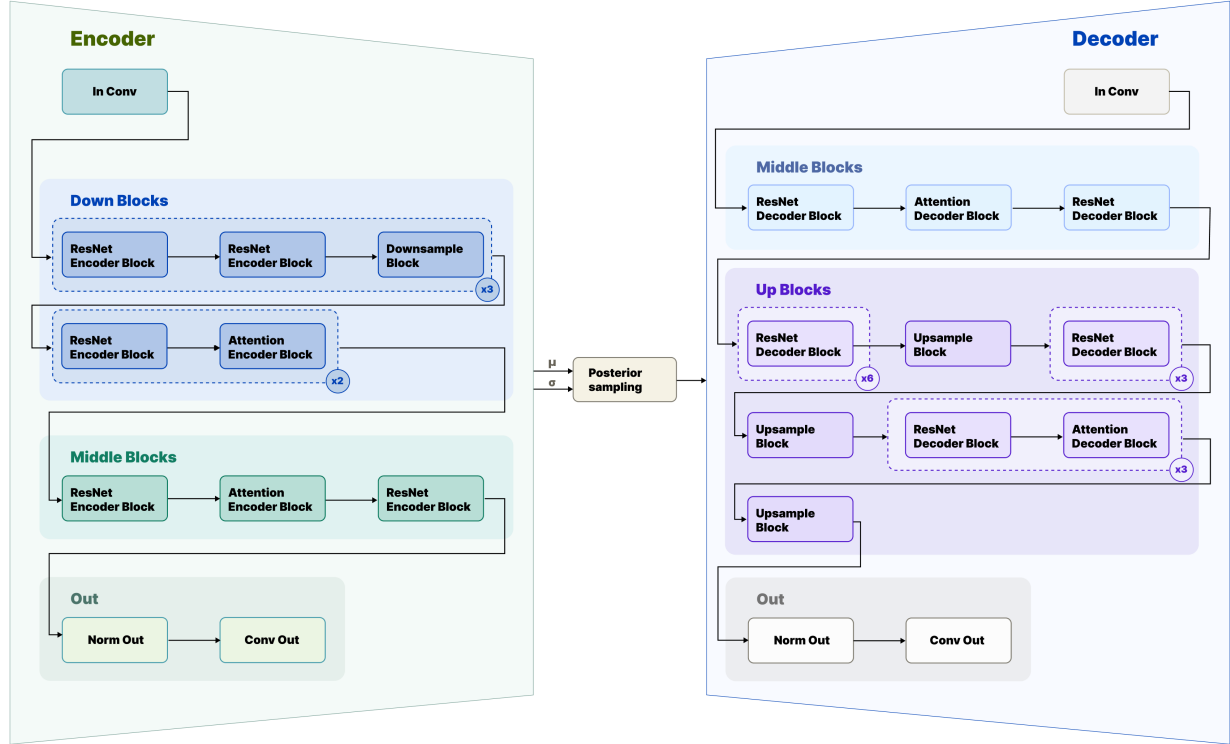


Figure 1: VAE architecture.

Perceptual Loss [19]. This is a feature matching loss, which is calculated via a distance metric using deep features Φ_l from pre-trained networks:

$$\mathcal{L}_{\text{perc}} = \mathbb{E}_{q_{\phi}(z|x)} \|\Phi_l(\mathbf{x}) - \Phi_l(\hat{\mathbf{x}})\|_1. \quad (6)$$

A popular choice for the perceptual loss is LPIPS [55].

Complete Objective. The total loss combines these components with weighting factors:

$$\mathcal{L}_{\text{total}} = \lambda_{\text{KL}} \mathcal{L}_{\text{KL}} + \lambda_{\text{recon}} \mathcal{L}_{\text{recon}} + \lambda_{\text{adv}} \mathcal{L}_{\text{adv}} + \lambda_{\text{perc}} \mathcal{L}_{\text{perc}}. \quad (7)$$

3.2 VAE architecture

Our base VAE architecture builds upon the open-source² SBER-MoVQGAN model [1], which itself is derived from VQGAN [12] and incorporates spatially conditional normalization from MoVQ [57]. In our implementation, we replace the quantization bottleneck with mean μ and log-variance $\log \sigma^2$ prediction layers to form a KL-VAE continuous latent space.

Figure 1 provides a detailed scheme of the KL-VAE structures. Following the design in [38], each encoder block consists of a ResNet Block [15] followed by a downscale module, with some layers additionally incorporating Self-Attention Blocks [48]. The decoder similarly employs ResNet blocks but replaces downscale modules with upscale operations, retaining self-attention where applicable. Detailed ResNet and Self-Attention block schemes are presented in Appendix A.1.

We also introduce minor architectural modifications to address the artifacts described in Section 4. We describe these changes in Section 5.2, other implementation details can be found in Appendix A.2.

3.3 Latent diffusion VAE

Latent diffusion models (LDMs) [38] perform diffusion processes in a compressed latent space rather than operating directly on high-dimensional input data (e.g., pixel space for images). By employing a variational autoencoder (VAE)

²<https://github.com/ai-forever/MoVQGAN>

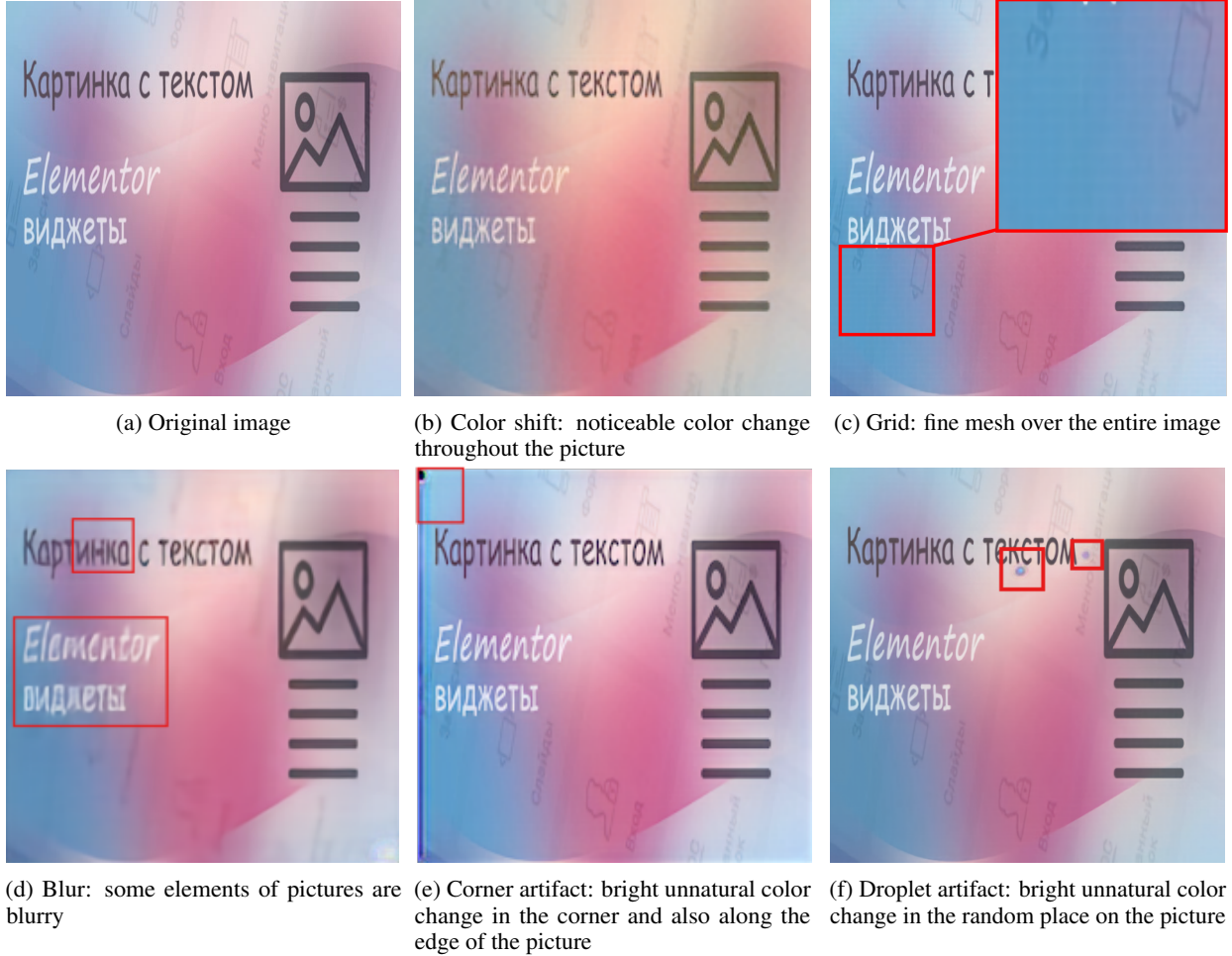


Figure 2: Reconstruction artifacts resulting from the unimproved VAE model.

to encode data into a lower-dimensional representation, LDMs achieve significant computational efficiency while maintaining high generation quality.

The VAE encoder transforms an input image $\mathbf{x} \in \mathbb{R}^{H \times W \times C}$ (with height H , width W , and channels C) into a latent representation $\mathbf{z} \in \mathbb{R}^{H/f \times W/f \times c}$, where f is the spatial downscaling factor and c denotes the increased channel dimension for information preservation. In transformer-based implementations [31], the quadratic complexity of full self-attention with respect to latents size makes spatial dimension operations particularly costly. Channel dimension adjustments, however, can be efficiently implemented through linear projections with minimal computational overhead.

In this work, we further investigate the suitability of our enhanced image reconstruction VAE in a latent diffusion pipeline for text-to-image generation. We employ a diffusion transformer based on LI-DiT [28], training it with our frozen VAE, and present the results in Section 6.3.

4 Image VAE challenges

Researchers frequently encounter challenges when training VAEs, yet most studies only report final configurations while omitting the methodological details of how they were achieved. Firstly, the difference in data collection can cause irreproducible results even for the full repetition of the training pipeline. Secondly, the extensive number of hyperparameters inherent in VAE training makes the learning process highly complex. Researchers must determine an appropriate combination of loss functions and carefully select hyperparameters for each training setup, for example, when increasing image resolution. Due to the interdependence of hyperparameters, suboptimal tuning can result in significant training difficulties and artifacts in reconstructed images. Finally, incorporating a discriminator in VAE training can introduce additional challenges, such as instability, vanishing gradients, and mode collapse. All

aforementioned issues often manifest as specific defects in VAE reconstructions. We argue that these defects can be systematically categorized based on their visual characteristics and underlying causes. Below, we provide an overview of common artifacts and their potential origins.

Color shift. The first artifact while training VAE with adversarial loss is a color shift. It manifests itself in the fact that the color of all generated images is moved towards one color. In our case all the pictures had a yellow tint. The example of this problem is presented in Figure 2b. This artifact appear at the early stages of training. One of the possible reasons of it is the adversarial training setup. Such problem can be considered as a kind of mode collapse.

Grid. One more unpleasant attribute which can occur in the reconstructed images while training VAE with the discriminator. The example of this problem is presented in Figure 2c. In our experiments, this problem arose when the adversarial loss had too much weight.

Blur. The most common artifact while training the VAE. Unlike the previous problems, its appearance is associated with the regularization of the latent space during training of the VAE with the KL divergence loss. This part of loss pushes posterior distribution to the $\mathcal{N}(\mathbf{0}, \mathbf{I})$ so the high weight for it can create too simple distribution of the latent variables and blurred reconstructions. The example of this problem is presented in Figure 2d.

Corner artifact. The next two problems are connected with the model architecture design. The first of them is the corner artifact. This artifact looks like a frame of blur around the edges of the image and presented in the Figure 2e. Explanation for this can be found in the convolutional layers in the architecture and particularly in padding used in them. In our experiments we found out that zero padding cause this problem.

Droplet artifact. This peculiarity was also mentioned in the [33]. The authors pointed out that this problem caused by the high norms in latent codes in certain spatial locations. After decoding these high norms produce the bright spots in the pixel space. In our work we also faced with this problem, the example is presented at the Figure 2f. Also the Figure 3 shows formation process of this artifact by displaying the activations norms for the different layers of the VAE decoder. To mitigate this problem the authors of the [33] invented an additional outlier loss, which penalizes the model for latent values far from the mean. We propose to solve this problem in other, simpler way.

5 Methods

This section describes the data selection and preprocessing methods, and presents our findings about on mitigating the problems of VAE training depicted in Section 4.

5.1 Data preprocessing

Data quality is a critical factor influencing the performance of VAE. Specifically, the training dataset should consist of high-resolution images exhibiting a substantial amount of high-frequency detail.

Another key consideration is data preprocessing, which typically involves resizing and cropping images to reduce their resolution. However, our experiments demonstrate that directly cropping high-resolution images (e.g., 720p or HD) to a

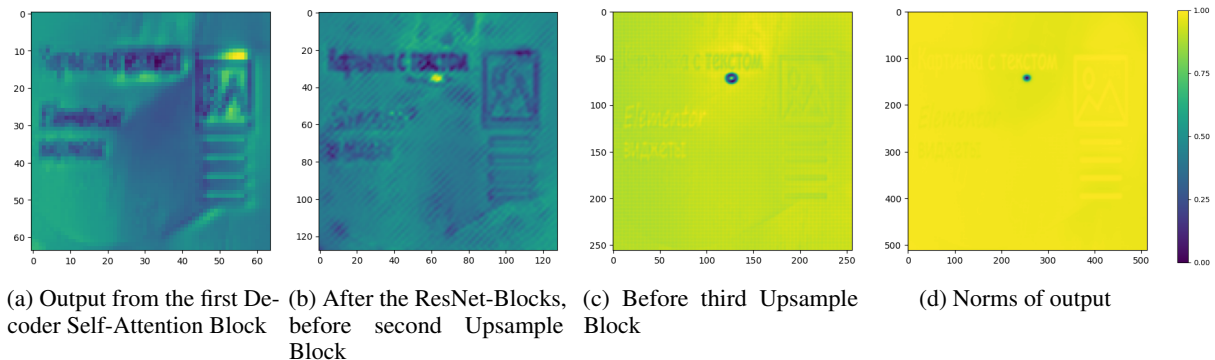


Figure 3: Droplet artifact formation. Activation norms grow on several consecutive Decoder layers.

lower resolution (e.g., 240p) can adversely affect VAE training. Such transformations yield images that are effectively magnified regions of the originals, lacking sufficient high-frequency information. Consequently, these images do not possess the representational complexity necessary for training a high-quality VAE. Instead, a more effective approach involves first proportionally resizing a large image to an intermediate resolution (e.g., $\sim 480p$) before cropping to the target resolution (e.g., 240p).

The resizing method also significantly impacts performance. Our experiments indicate that the default nearest-neighbor method yields suboptimal results, whereas the bicubic method produces superior outcomes. These findings align with established results from prior work [14, 4]. Notably, training a VAE on lower-resolution images (e.g., 240p) can remain effective for operation at higher resolutions (e.g., 480p or 720p), as the convolutional receptive field remains unchanged. Thus, the VAE learns to compress the image by a factor of n along each side in the same manner as with smaller resolutions.

Our complete training dataset consists of 100 million images sourced from the publicly available LAION Aesthetic HighRes dataset, a subset of LAION-5B [40]. All images in this dataset have HD resolution and an associated aesthetic score. We selected only images with a score > 4.5 , resized them from HD to 480p, and then cropped them to 240p.

5.2 Challenges solutions

Color shift. This problem is very common and can occur in many different situations. Often this artifact reveals itself in the early steps of training and indicates that the model has not been fully trained. This problem is solved in two ways: either prolonged training of the whole model or only training the decoder part.

Grid. As it was said in previous section this unpleasant artifact that occurred due to the large weight on the discriminator. So, this problem can be reduced by the lowering this weight.

Blur. As this the most common problem with VAE, arising due to the very essence of KL regularization of the latent space. It can be solved by reducing the weight for the regularization term and increasing the weight on the discriminator. But such solution contradict with the previous artifact. Therefore it is very important to choose the right weight for the discriminator and the KL regularization term. In our case, decreasing weight of KL divergence by 10 times solved the problem.

Corner artifact. This undesirable artifact as it was said above appears due to the zero padding in the convolutions layers of the VAE. Actually, one can not to face with such issue because many open source architectures use this type of padding and do not obtain similar problem. But in our work we uncover that this picture deterioration is completely cured by changing the padding type to reflect.

Droplet artifact. At first this artifact appeared in the corner and we assumed that it also appeared due to incorrect padding and that we would get rid of it with the previous artifact after padding changing. But after that the dot began to move throughout the whole picture. As it was already mentioned the real reason is the high norms in activations during decoding. Unlike the [33] we decided not to add the new loss term, as it would make the total loss more complicated and hard to adjust its weights, but make changes to the architecture of the model. We use the method proposed in [57] named Spatially Conditional Normalization. The authors used this normalization to modulate the quantized vectors so as to insert spatially variant information to the embedded index maps. In this way, they achieved a reduction in the number of artifacts that arise due to encoding similar patches into one latent codebook vector. For us this layer has two main benefits. First, it acts as a supplementary normalization layer. Second, it provides additional spatial interactions between parts of the image. And although we are not working with a discrete latent space, using this layer helps us get rid of the droplet artifact.

5.3 Decoder finetuning

Another sufficient step to improve VAE reconstruction quality is a freezing of encoder. This training stage can further improve quality of trained model and help to get rid of other artifacts. In our experiments, an additional training phase with a fixed encoder helped us further increase the FID metric at a late phase of training. Similar strategy was used for example in [13] where the stage with frozen encoder was even longer than full VAE training stage.

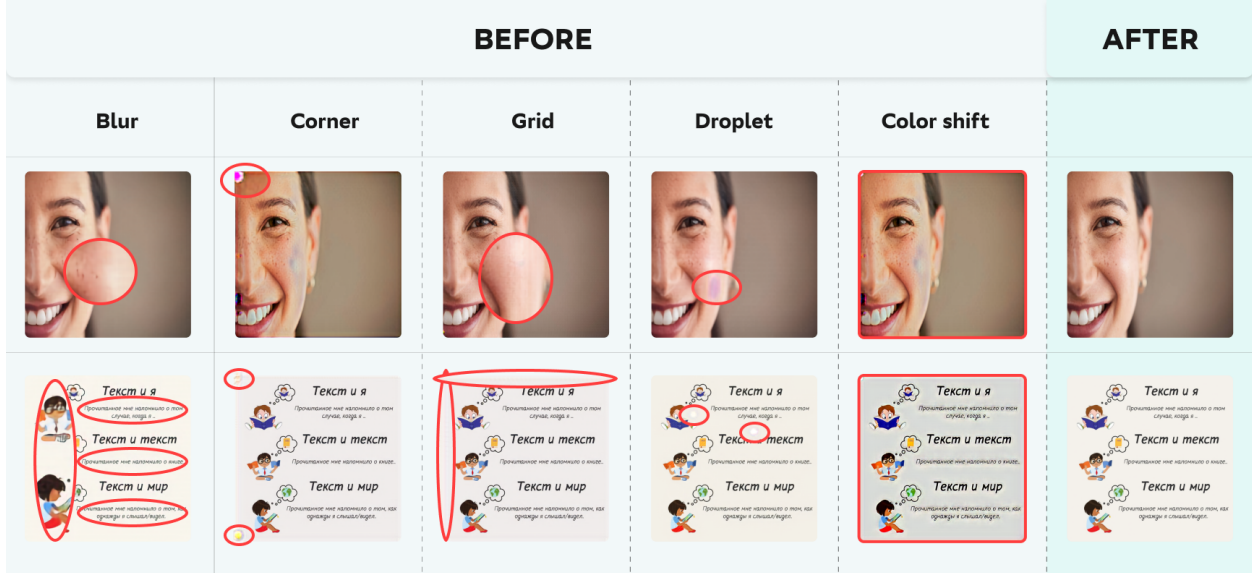


Figure 4: The results of our methods for addressing VAE reconstruction artifacts. Our proposed approach effectively eliminates many problems, ensuring high-quality reconstructions.

6 Results

6.1 Artifact mitigation

We applied the techniques described in Section 5.2 and trained VAE model on the dataset described in Section 5.1 and with the training parameters that can be found in Appendix A.2. We conducted a qualitative comparison between new model and the base VAE model described in Section 3.2. The results are presented in Figure 4. As can be clearly seen, our approach effectively eliminates all artifacts listed in Section 4. More examples can be found in Appendix B.

6.2 Image reconstruction

To assess the reconstruction performance of our approach, we employ two standard metrics: peak signal-to-noise ratio (PSNR) and structural similarity index measure (SSIM). We evaluate these metrics on multiple benchmark datasets, including ImageNet³ [9] at resolutions of 256×256 and 512×512 , MS COCO 2017 Test⁴ [27] at 512×512 , and FFHQ⁵ [20] at 1024×1024 .

For comparison, we test our model against several state-of-the-art autoencoders: DC-VAE [6], Cosmos-0.1-Tokenizer-CI8 \times 8⁶ [29], Flux VAE⁷ [25], and the VAE from Stable Diffusion 3 [11]. The quantitative results, presented in Table 1, demonstrate that our method achieves state-of-the-art performance in image reconstruction, attaining the highest – or competitively equivalent – scores in both SSIM and PSNR across all evaluated datasets. This quantitative superiority is further supported by qualitative evaluation, as illustrated in Figure 5, where our method exhibits competitive results compared to the best approaches.

6.3 Text-to-image generation

To assess the integration of our VAE with latent diffusion pipeline, we train a Diffusion Transformer (DiT), which is similar to LI-DiT model [28]. The architecture consists of two principal components:

- Token Refiner that processes textual embeddings through self-attention and feed-forward layers with Adaptive Layer Normalization (AdaNorm) [51] for temporal conditioning;

³<https://www.image-net.org/challenges/LSVRC/2012/>

⁴<https://cocodataset.org/>

⁵<https://github.com/NVLabs/ffhq-dataset>

⁶<https://huggingface.co/nvidia/Cosmos-0.1-Tokenizer-CI8x8>

⁷<https://huggingface.co/black-forest-labs/FLUX.1-dev>

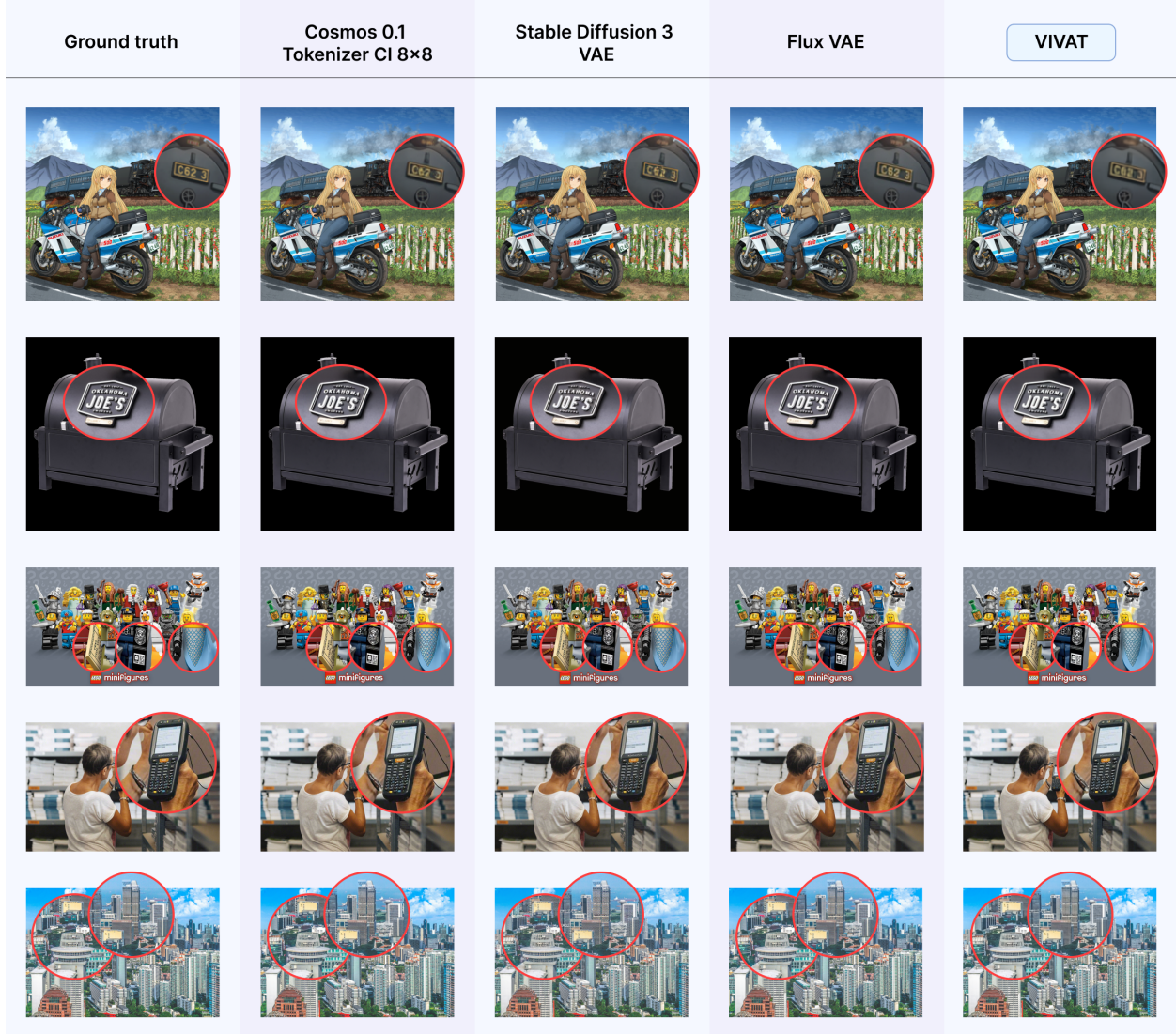


Figure 5: The results of image reconstruction using different models. A zoom-in shows that our approach, based on simple heuristics, leads to the results compared to state-of-the-art models. By artifacts mitigation, it is possible to achieve higher quality in the reconstruction of small details and text.

- Cross-Attention Block that handles visual embeddings via self-attention while enabling text conditioning through cross-attention mechanisms and employing AdaNorm for temporal information.

For comparative evaluation between VIVAT and Flux VAE [25], we trained a 2 billion parameter DiT model for 130 thousand steps on 256×256 resolution images with a batch size of 1024. Generation quality was quantified using the CLIP-score metric [16] to measure text-image alignment. Figure 6 shows that our method allows for a stable improvement in quality during the training process and surpasses the pipeline with the same diffusion transformer, but using Flux VAE. Details of the architecture and training of the diffusion transformer can be found in Appendix A.3.

7 Conclusion

In this work, we identified and addressed key challenges in KL-VAE training through a systematic analysis of artifacts and their mitigation. By refining loss weightings, architectural details, and training strategies, VIVAT achieves superior reconstruction quality and enhances performance of the latent diffusion pipeline for text-to-image generation. Our approach demonstrates that significant improvements can be made without departing from the classical VAE framework,

Table 1: Image reconstruction results. The best values are **highlighted**, and the second-best values are underlined.

Model	ImageNet 256 × 256	ImageNet 512 × 512	MS COCO 2017 Test 512 × 512	FFHQ 1024 × 1024
PSNR↑				
DC-VAE	23.7	26.15	25.38	31.34
Cosmos-0.1-Tokenizer-CI8×8	30.54	33.76	32.28	<u>39.12</u>
Flux VAE	<u>31.09</u>	33.99	32.65	38.14
Stable Diffusion 3 VAE	29.58	32.07	30.94	36.16
VIVAT (Our)	31.25	<u>33.82</u>	<u>32.61</u>	39.35
SSIM↑				
DC-VAE	0.65	0.71	0.70	0.83
Cosmos-0.1-Tokenizer-CI8x8	0.88	0.91	0.90	0.95
Flux VAE	<u>0.89</u>	0.93	0.91	0.96
Stable Diffusion 3 VAE	0.86	0.89	0.87	0.93
VIVAT (Our)	0.90	<u>0.92</u>	0.91	0.96

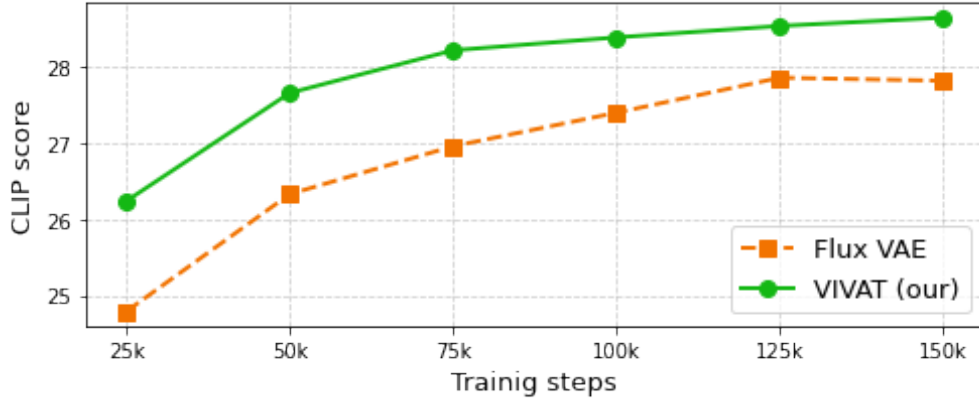


Figure 6: The CLIP score on the validation dataset during the training process of the diffusion transformer with image embeddings obtained from Flux VAE or our method VIVAT. Our method shows a stable improvement in text-image alignment and outperforms the competitive method.

offering a practical and scalable solution for real-world applications. The success of VIVAT underscores the untapped potential of traditional autoencoding methods when combined with targeted optimizations. Future work could explore the extension of these principles to other generative tasks and architectures, including VAE for video generation pipelines.

Acknowledgments

The authors express the gratitude to Evelina Sidorova for her assistance in preparing the illustrations for this paper.

References

- [1] Vladimir Arkhipkin, Andrei Filatov, Viacheslav Vasilev, Anastasia Maltseva, Said Azizov, Igor Pavlov, Julia Agafonova, Andrey Kuznetsov, and Denis Dimitrov. 2024. Kandinsky 3.0 Technical Report. arXiv:2312.03511 [cs.CV] <https://arxiv.org/abs/2312.03511>
- [2] Vladimir Arkhipkin, Zein Shaheen, Viacheslav Vasilev, Elizaveta Dakhova, Konstantin Sobolev, Andrey Kuznetsov, and Denis Dimitrov. 2025. ImproveYourVideos: Architectural Improvements for Text-to-Video Generation Pipeline. *IEEE Access* 13 (2025), 1986–2003. doi:10.1109/ACCESS.2024.3522510
- [3] Shuai Bai, Keqin Chen, Xuejing Liu, Jialin Wang, Wenbin Ge, Sibong Song, Kai Dang, Peng Wang, Shijie Wang, Jun Tang, et al. 2025. Qwen2. 5-vl technical report.

- [4] Parth Bhatt and Rakesh Pandit. 2013. Comparative Analysis of Interpolation and Texture Synthesis Method for Enhancing Image.
- [5] Andreas Blattmann, Robin Rombach, Huan Ling, Tim Dockhorn, Seung Wook Kim, Sanja Fidler, and Karsten Kreis. 2023. Align your Latents: High-Resolution Video Synthesis with Latent Diffusion Models.
- [6] Junyu Chen, Han Cai, Junsong Chen, Enze Xie, Shang Yang, Haotian Tang, Muyang Li, Yao Lu, and Song Han. 2025. Deep Compression Autoencoder for Efficient High-Resolution Diffusion Models. arXiv:2410.10733 [cs.CV] <https://arxiv.org/abs/2410.10733>
- [7] Junsong Chen, Jincheng Yu, Chongjian Ge, Lewei Yao, Enze Xie, Yue Wu, Zhongdao Wang, James Kwok, Ping Luo, Huchuan Lu, and Zhenguo Li. 2023. PixArt- α : Fast Training of Diffusion Transformer for Photorealistic Text-to-Image Synthesis. arXiv:2310.00426 [cs.CV]
- [8] Rewon Child. 2021. Very Deep VAEs Generalize Autoregressive Models and Can Outperform Them on Images. arXiv:2011.10650 [cs.LG] <https://arxiv.org/abs/2011.10650>
- [9] Jia Deng, Wei Dong, Richard Socher, Li-Jia Li, Kai Li, and Li Fei-Fei. 2009. ImageNet: A large-scale hierarchical image database. 248-255 pages. doi:10.1109/CVPR.2009.5206848
- [10] Nat Dilokthanakul, Pedro A. M. Mediano, Marta Garnelo, Matthew C. H. Lee, Hugh Salimbeni, Kai Arulkumaran, and Murray Shanahan. 2017. Deep Unsupervised Clustering with Gaussian Mixture Variational Autoencoders. arXiv:1611.02648 [cs.LG] <https://arxiv.org/abs/1611.02648>
- [11] Patrick Esser, Sumith Kulal, Andreas Blattmann, Rahim Entezari, Jonas Müller, Harry Saini, Yam Levi, Dominik Lorenz, Axel Sauer, Frederic Boesel, Dustin Podell, Tim Dockhorn, Zion English, Kyle Lacey, Alex Goodwin, Yannik Marek, and Robin Rombach. 2024. Scaling Rectified Flow Transformers for High-Resolution Image Synthesis. arXiv:2403.03206 [cs.CV] <https://arxiv.org/abs/2403.03206>
- [12] Patrick Esser, Robin Rombach, and Björn Ommer. 2020. Taming Transformers for High-Resolution Image Synthesis. arXiv:2012.09841 [cs.CV]
- [13] Zach Evans, CJ Carr, Josiah Taylor, Scott H. Hawley, and Jordi Pons. 2024. Fast Timing-Conditioned Latent Audio Diffusion. arXiv:2402.04825 [cs.SD] <https://arxiv.org/abs/2402.04825>
- [14] Dianyuan Han. 2013. Comparison of Commonly Used Image Interpolation Methods. 1556-1559 pages. doi:10.2991/iccsee.2013.391
- [15] Kaiming He, Xiangyu Zhang, Shaoqing Ren, and Jian Sun. 2015. Deep Residual Learning for Image Recognition. arXiv:1512.03385 [cs.CV] <https://arxiv.org/abs/1512.03385>
- [16] Jack Hessel, Ari Holtzman, Maxwell Forbes, Ronan Le Bras, and Yejin Choi. 2021. CLIPScore: A Reference-free Evaluation Metric for Image Captioning. <https://api.semanticscholar.org/CorpusID:233296711>
- [17] Irina Higgins, Loïc Matthey, Arka Pal, Christopher P. Burgess, Xavier Glorot, Matthew M. Botvinick, Shakir Mohamed, and Alexander Lerchner. 2016. beta-VAE: Learning Basic Visual Concepts with a Constrained Variational Framework. <https://api.semanticscholar.org/CorpusID:46798026>
- [18] Liming Jiang, Bo Dai, Wayne Wu, and Chen Change Loy. 2021. Focal Frequency Loss for Image Reconstruction and Synthesis. arXiv:2012.12821 [cs.CV] <https://arxiv.org/abs/2012.12821>
- [19] Justin Johnson, Alexandre Alahi, and Li Fei-Fei. 2016. Perceptual Losses for Real-Time Style Transfer and Super-Resolution. arXiv:1603.08155 [cs.CV] <https://arxiv.org/abs/1603.08155>
- [20] Tero Karras, Samuli Laine, and Timo Aila. 2019. A Style-Based Generator Architecture for Generative Adversarial Networks. arXiv:1812.04948 [cs.NE] <https://arxiv.org/abs/1812.04948>
- [21] Diederik P Kingma and Max Welling. 2013. Auto-Encoding Variational Bayes. arXiv:1312.6114 [stat.ML] <https://arxiv.org/abs/1312.6114>
- [22] Diederik P. Kingma and Max Welling. 2019. An Introduction to Variational Autoencoders. *Foundations and Trends® in Machine Learning* 12, 4 (2019), 307–392. doi:10.1561/22000000056
- [23] Weijie Kong, Qi Tian, Zijian Zhang, Rox Min, Zuozhuo Dai, Jin Zhou, Jiangfeng Xiong, Xin Li, Bo Wu, Jianwei Zhang, Kathrina Wu, Qin Lin, Junkun Yuan, Yanxin Long, Aladdin Wang, Andong Wang, Changlin Li, Duojuan Huang, Fang Yang, Hao Tan, Hongmei Wang, Jacob Song, Jiawang Bai, Jianbing Wu, Jinbao Xue, Joey Wang, Kai Wang, Mengyang Liu, Pengyu Li, Shuai Li, Weiyang Wang, Wenqing Yu, Xincheng Deng, Yang Li, Yi Chen, Yutao Cui, Yuanbo Peng, Zhentao Yu, Zhiyu He, Zhiyong Xu, Zixiang Zhou, Zunnan Xu, Yangyu Tao, Qinglin Lu, Songtao Liu, Dax Zhou, Hongfa Wang, Yong Yang, Di Wang, Yuhong Liu, Jie Jiang, and Caesar Zhong. 2025. HunyuanVideo: A Systematic Framework For Large Video Generative Models. arXiv:2412.03603 [cs.CV] <https://arxiv.org/abs/2412.03603>

- [24] Theodoros Kozelias, Ioannis Kakogeorgiou, Spyros Gidaris, and Nikos Komodakis. 2025. EQ-VAE: Equivariance Regularized Latent Space for Improved Generative Image Modeling. arXiv:2502.09509 [cs.LG] <https://arxiv.org/abs/2502.09509>
- [25] Black Forest Labs. 2024. FLUX. <https://github.com/black-forest-labs/flux>.
- [26] Anders Boesen Lindbo Larsen, Søren Kaae Sønderby, Hugo Larochelle, and Ole Winther. 2016. Autoencoding beyond pixels using a learned similarity metric. arXiv:1512.09300 [cs.LG] <https://arxiv.org/abs/1512.09300>
- [27] Tsung-Yi Lin, Michael Maire, Serge Belongie, Lubomir Bourdev, Ross Girshick, James Hays, Pietro Perona, Deva Ramanan, C. Lawrence Zitnick, and Piotr Dollár. 2015. Microsoft COCO: Common Objects in Context. arXiv:1405.0312 [cs.CV] <https://arxiv.org/abs/1405.0312>
- [28] Bingqi Ma, Zhuofan Zong, Guanglu Song, Hongsheng Li, and Yu Liu. 2024. Exploring the role of large language models in prompt encoding for diffusion models.
- [29] NVIDIA. 2025. Cosmos World Foundation Model Platform for Physical AI. arXiv:2501.03575 [cs.CV] <https://arxiv.org/abs/2501.03575>
- [30] Kushagra Pandey, Avideep Mukherjee, Piyush Rai, and Abhishek Kumar. 2022. DiffuseVAE: Efficient, Controllable and High-Fidelity Generation from Low-Dimensional Latents. arXiv:2201.00308 [cs.LG] <https://arxiv.org/abs/2201.00308>
- [31] William Peebles and Saining Xie. 2023. Scalable Diffusion Models with Transformers. arXiv:2212.09748 [cs.CV] <https://arxiv.org/abs/2212.09748>
- [32] Dustin Podell, Zion English, Kyle Lacey, Andreas Blattmann, Tim Dockhorn, Jonas Müller, Joe Penna, and Robin Rombach. 2023. SDXL: Improving Latent Diffusion Models for High-Resolution Image Synthesis. arXiv:2307.01952 [cs.CV] <https://arxiv.org/abs/2307.01952>
- [33] Adam Polyak et al. 2024. Movie Gen: A Cast of Media Foundation Models. arXiv:2410.13720 [cs.CV] <https://arxiv.org/abs/2410.13720>
- [34] Alec Radford, Jong Wook Kim, Chris Hallacy, Aditya Ramesh, Gabriel Goh, Sandhini Agarwal, Girish Sastry, Amanda Askell, Pamela Mishkin, Jack Clark, et al. 2021. Learning transferable visual models from natural language supervision. 8748–8763 pages.
- [35] Aditya Ramesh, Prafulla Dhariwal, Alex Nichol, Casey Chu, and Mark Chen. 2022. Hierarchical Text-Conditional Image Generation with CLIP Latents. arXiv:2204.06125 [cs.CV] <https://arxiv.org/abs/2204.06125>
- [36] Ali Razavi, Aaron van den Oord, and Oriol Vinyals. 2019. Generating Diverse High-Fidelity Images with VQ-VAE-2. arXiv:1906.00446 [cs.LG] <https://arxiv.org/abs/1906.00446>
- [37] Danilo Jimenez Rezende, Shakir Mohamed, and Daan Wierstra. 2014. Stochastic Backpropagation and Approximate Inference in Deep Generative Models. In *Proceedings of the 31st International Conference on Machine Learning (Proceedings of Machine Learning Research, Vol. 32)*, Eric P. Xing and Tony Jebara (Eds.). PMLR, Beijing, China, 1278–1286. <https://proceedings.mlr.press/v32/rezende14.html>
- [38] Robin Rombach, Andreas Blattmann, Dominik Lorenz, Patrick Esser, and Björn Ommer. 2022. High-Resolution Image Synthesis with Latent Diffusion Models. arXiv:2112.10752 [cs.CV] <https://arxiv.org/abs/2112.10752>
- [39] Oleh Rybkin, Kostas Daniilidis, and Sergey Levine. 2021. Simple and Effective VAE Training with Calibrated Decoders. 9179–9189 pages. <https://proceedings.mlr.press/v139/rybkin21a.html>
- [40] Christoph Schuhmann, Romain Beaumont, Richard Vencu, Cade Gordon, Ross Wightman, Mehdi Cherti, Theo Coombes, Aarush Katta, Clayton Mullis, Mitchell Wortsman, et al. 2022. Laion-5b: An open large-scale dataset for training next generation image-text models. *Advances in neural information processing systems* 35 (2022), 25278–25294.
- [41] Samarth Sinha and Adji B. Dieng. 2021. Consistency regularization for variational auto-encoders. In *Proceedings of the 35th International Conference on Neural Information Processing Systems (NIPS '21)*. Curran Associates Inc., Red Hook, NY, USA, Article 991, 12 pages.
- [42] Ivan Skorokhodov, Sharath Girish, Benran Hu, Willi Menapace, Yanyu Li, Rameen Abdal, Sergey Tulyakov, and Aliaksandr Siarohin. 2025. Improving the Diffusability of Autoencoders. arXiv:2502.14831 [cs.CV] <https://arxiv.org/abs/2502.14831>
- [43] Hiroshi Takahashi, Tomoharu Iwata, Yuki Yamanaka, Masanori Yamada, and Satoshi Yagi. 2019. Variational autoencoder with implicit optimal priors. 8 pages. doi:10.1609/aaai.v33i01.33015066

- [44] Ilya Tolstikhin, Olivier Bousquet, Sylvain Gelly, and Bernhard Schoelkopf. 2019. Wasserstein Auto-Encoders. arXiv:1711.01558 [stat.ML] <https://arxiv.org/abs/1711.01558>
- [45] Michael Tschannen, Cian Eastwood, and Fabian Mentzer. 2025. GIVT: Generative Infinite-Vocabulary Transformers. In *Computer Vision – ECCV 2024*, Aleš Leonardis, Elisa Ricci, Stefan Roth, Olga Russakovsky, Torsten Sattler, and Gül Varol (Eds.). Springer Nature Switzerland, Cham, 292–309.
- [46] Arash Vahdat and Jan Kautz. 2021. NVAE: A Deep Hierarchical Variational Autoencoder. arXiv:2007.03898 [stat.ML] <https://arxiv.org/abs/2007.03898>
- [47] Aaron van den Oord, Oriol Vinyals, and Koray Kavukcuoglu. 2017. Neural discrete representation learning. In *Proceedings of the 31st International Conference on Neural Information Processing Systems (Long Beach, California, USA) (NIPS’17)*. Curran Associates Inc., Red Hook, NY, USA, 6309–6318.
- [48] Ashish Vaswani, Noam Shazeer, Niki Parmar, Jakob Uszkoreit, Llion Jones, Aidan N. Gomez, Łukasz Kaiser, and Illia Polosukhin. 2017. Attention is all you need. In *Proceedings of the 31st International Conference on Neural Information Processing Systems (Long Beach, California, USA) (NIPS’17)*. Curran Associates Inc., Red Hook, NY, USA, 6000–6010.
- [49] Arkhipkin Vladimir, Viacheslav Vasilev, Andrei Filatov, Igor Pavlov, Julia Agafonova, Nikolai Gerasimenko, Anna Averchenkova, Evelina Mironova, Bukashkin Anton, Konstantin Kulikov, Andrey Kuznetsov, and Denis Dimitrov. 2024. Kandinsky 3: Text-to-Image Synthesis for Multifunctional Generative Framework. In *Proceedings of the 2024 Conference on Empirical Methods in Natural Language Processing: System Demonstrations*, Delia Irazu Hernandez Farias, Tom Hope, and Manling Li (Eds.). Association for Computational Linguistics, Miami, Florida, USA, 475–485. doi:10.18653/v1/2024.emnlp-demo.48
- [50] Yuxin Wu and Kaiming He. 2018. Group Normalization. arXiv:1803.08494 [cs.CV] <https://arxiv.org/abs/1803.08494>
- [51] Jingjing Xu, Xu Sun, Zhiyuan Zhang, Guangxiang Zhao, and Junyang Lin. 2019. Understanding and Improving Layer Normalization. arXiv:1911.07013 [cs.LG] <https://arxiv.org/abs/1911.07013>
- [52] Xinchun Yan, Jimei Yang, Kihyuk Sohn, and Honglak Lee. 2016. Attribute2Image: Conditional Image Generation from Visual Attributes. In *Computer Vision – ECCV 2016*, Bastian Leibe, Jiri Matas, Nicu Sebe, and Max Welling (Eds.). Springer International Publishing, Cham, 776–791.
- [53] Zhuoyi Yang, Jiayan Teng, Wendi Zheng, Ming Ding, Shiyu Huang, Jiazheng Xu, Yuanming Yang, Wenyi Hong, Xiaohan Zhang, Guanyu Feng, Da Yin, Yuxuan Zhang, Weihang Wang, Yean Cheng, Bin Xu, Xiaotao Gu, Yuxiao Dong, and Jie Tang. 2025. CogVideoX: Text-to-Video Diffusion Models with An Expert Transformer. arXiv:2408.06072 [cs.CV] <https://arxiv.org/abs/2408.06072>
- [54] Jiahui Yu, Xin Li, Jing Yu Koh, Han Zhang, Ruoming Pang, James Qin, Alexander Ku, Yuanzhong Xu, Jason Baldridge, and Yonghui Wu. 2022. Vector-quantized Image Modeling with Improved VQGAN. arXiv:2110.04627 [cs.CV] <https://arxiv.org/abs/2110.04627>
- [55] Richard Zhang, Phillip Isola, Alexei A. Efros, Eli Shechtman, and Oliver Wang. 2018. The Unreasonable Effectiveness of Deep Features as a Perceptual Metric. arXiv:1801.03924 [cs.CV] <https://arxiv.org/abs/1801.03924>
- [56] Jake Zhao, Yoon Kim, Kelly Zhang, Alexander M. Rush, and Yann LeCun. 2018. Adversarially Regularized Autoencoders. arXiv:1706.04223 [cs.LG] <https://arxiv.org/abs/1706.04223>
- [57] Chuanxia Zheng, Long Tung Vuong, Jianfei Cai, and Dinh Phung. 2022. MoVQ: modulating quantized vectors for high-fidelity image generation. In *Proceedings of the 36th International Conference on Neural Information Processing Systems (New Orleans, LA, USA) (NIPS ’22)*. Curran Associates Inc., Red Hook, NY, USA, Article 1701, 14 pages.

A Implementation Details

A.1 VAE Blocks

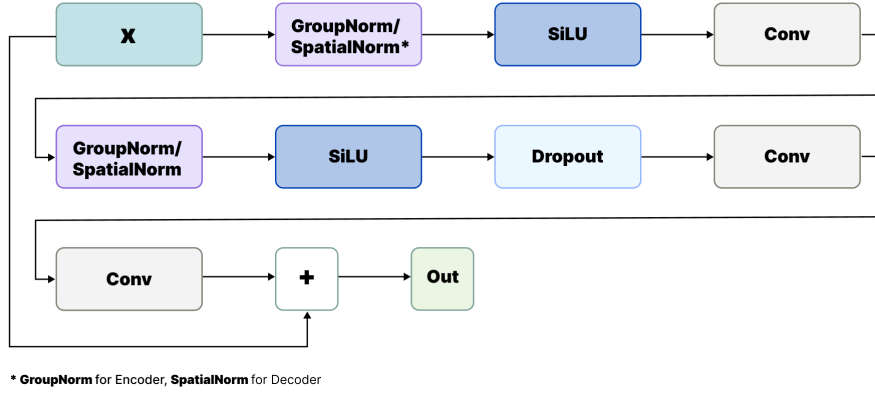


Figure 7: The ResNet Block for the VAE Encoder or Decoder. We use the Group Normalization [50] for the Encoder and Spatially Conditional Normalization [57] for the Decoder.

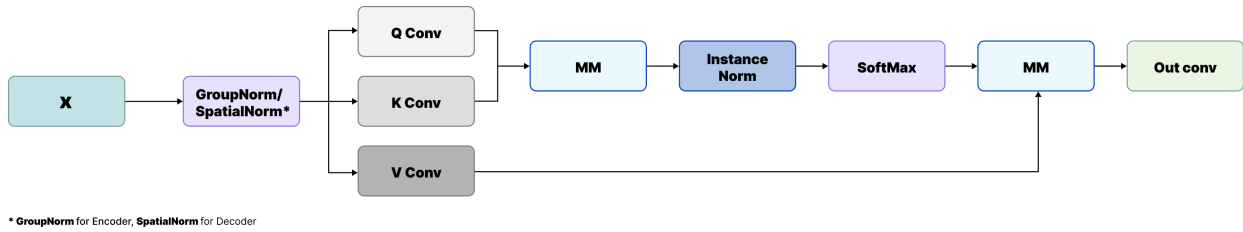


Figure 8: The Self-Attention Block for the VAE Encoder or Decoder. We use the Group Normalization [50] for the Encoder and Spatially Conditional Normalization [57] for the Decoder.

A.2 VAE Training

Our variational autoencoder was implemented with the configuration presented in the Table 2.

Table 2: VAE training parameters

Parameter	Value
Precision	FP32
Learning rate (η)	1×10^{-4}
EMA decay (γ)	0.9999
Latent dimension (d_z)	16
Discriminator start	Step 0

The optimal loss weights are presented in the Table 3.

Table 3: VAE losses coefficients

Component	Weight (λ)
KL Divergence Loss	1×10^{-4}
L_2 Reconstruction Loss	1.0
Adversarial Loss	0.01
Perceptual Loss	0.1

A.3 Diffusion Transformer (DiT)

The 2 billion parameter diffusion transformer employed the following architecture:

A.3.1 Embedding Systems

- **Qwen 2.5 VL 7B Instruct** [3]:
 - Embedding dimension: $d_{\text{Qwen}} = 3584$
 - Context length: $L_{\text{Qwen}} = 256$
- **CLIP** [34]:
 - Embedding dimension: $d_{\text{CLIP}} = 768$
 - Context length: $L_{\text{CLIP}} = 77$

A.3.2 Model Architecture

- Latent patch size: 2×2
- Time embedding dimension: $d_t = 512$
- Hidden dimension: $d_h = 1792$
- Feed-forward dimension: $d_{ff} = 7168$
- Transformer blocks: $N = 32$

A.3.3 Optimization Parameters

Table 4: Training Configuration

Parameter	Value
Optimizer	AdamW
Learning rate (η)	1×10^{-4}
Gradient clipping	$\ \nabla\ _2 \leq 1.0$
Weight decay	0.0
β_1, β_2	0.9, 0.95
ϵ	1×10^{-8}
LR schedule	Constant + 1000 warmup

B Additional Results on Artifact Mitigation

